applied sciences

MDPI

Article

Electronically Tunable Current Controlled Current Conveyor Transconductance Amplifier-Based Mixed-Mode Biquadratic Filter with Resistorless and Grounded Capacitors

Hua-Pin Chen [1,*] and Wan-Shing Yang [2]

1 Department of Electronic Engineering, Ming Chi University of Technology, New Taipei 24301, Taiwan
2 Department of Computer and Communication Engineering, De Lin Institute of Technology, New Taipei 23654, Taiwan; yang@dlit.edu.tw
* Correspondence: hpchen@mail.mcut.edu.tw; Tel.: +886-22-908-9899; Fax: +886-22-908-5247

Academic Editor: Hung-Yu Wang
Received: 22 December 2016; Accepted: 1 March 2017; Published: 4 March 2017

Abstract: A new electronically tunable mixed-mode biquadratic filter with three current controlled current conveyor transconductance amplifiers (CCCCTAs) and two grounded capacitors is proposed. With current input, the filter can realise lowpass (LP), bandpass (BP), highpass (HP), bandstop (BS) and allpass (AP) responses in current mode and LP, BP and HP responses in transimpedance mode. With voltage input, the filter can realise LP, BP, HP, BS and AP responses in voltage and transadmittance modes. Other attractive features of the mixed-mode biquadratic filter are (1) the use of two grounded capacitors, which is ideal for integrated circuit implementation; (2) orthogonal control of the quality factor (Q) and resonance angular frequency (ω_o) for easy electronic tenability; (3) low input impedance and high output impedance for current signals; (4) high input impedance for voltage signal; (5) avoidance of need for component-matching conditions; (6) resistorless and electronically tunable structure; (7) low active and passive sensitivities; and (8) independent control of the voltage transfer gains without affecting the parameters ω_o and Q.

Keywords: mixed-mode circuit; analogue electronics; filters; CCCCTA; electronically tunable

1. Introduction

Current-mode active elements have attracted the attention of analogue circuit designers because of their advantages over conventional operational amplifiers, which include higher accuracy, wider frequency response, larger dynamic range, greater linearity, lower power consumption and simpler implementation [1,2]. Thus, applications and advantages of various active filter transfer functions that use different active elements have been studied intensively [3–12]. Depending on the nature of input and output signals, filters are classified as current-mode (CM), voltage-mode (VM), transadmittance-mode (TAM) and transimpedance-mode (TIM) filters. In a VM structure, both input and output signals are voltages while in a CM structure, both input and output signals are currents. The TAM and TIM structures can function as bridges for transferring VM to CM and vice versa. Hence, mixed-mode circuits are worthy of study. Many types of mixed-mode circuits have been developed [13–27], utilizing assorted types of active elements such as conventional second-generation current conveyors (CCIIs) [13,14], current feedback operational amplifiers (CFOAs) [15], differential voltage current conveyors (DVCCs) [16], differential difference current conveyors (DDCCs) [17], fully differential current conveyors (FDCCIIs) [18], four-terminal floating nullors (FTFNs) [19], operational transconductance amplifiers (OTAs) [20–22], current controlled current conveyors (CCCIIs) [23–25], and current controlled current conveyor transconductance amplifiers (CCCCTAs) [26,27]. High performance electronically tunable active components have also received much attention. In CCCII and OTA, X-port parasitic resistance R_X and transconductance gain g_m, that are electronically controllable by the input bias currents I_S and I_B, respectively, have become the most promising active elements in the field of analogue circuit design. Thus, several electronically tunable mixed-mode biquadratic filters have been presented in the literature [20–25]. In the literature, circuits with different filter responses are realised according to the selected input signals, and they usually require two/three voltage signals for realising bandstop/allpass (BS/AP) filters and hence other active elements are needed to duplicate the input voltage signals. An attractive feature of multifunction active biquadratic filters is that lowpass (LP), bandpass (BP) and highpass (HP) outputs are simultaneously available in various circuit modes. These additional outputs can be used in systems that employ more than one filter function. Circuits that simultaneously use LP, BP and HP filters have applications in crossover networks used in three-way high-fidelity loudspeakers, touch-tone telephone systems and phase-locked loop frequency modulation stereo demodulators [12]. Simultaneously obtaining various filter functions in the same circuit topology increases the flexibility and versatility of practical applications.

Although several electronically tunable mixed-mode multifunction biquads with multiple-output current controlled conveyors (MOCCCIIs) and two grounded capacitors have been proposed [23–25], these circuits [24,25] suffer from the high-input impedance terminal in both VM and TAM. One interesting solution is the electronically tunable mixed-mode circuit [26]. Three CCCCTAs and two grounded capacitors were used to realise LP, BP and HP responses in all four modes in the same configuration. Both BS and AP responses can be realised in CM and TAM, but the AP response in CM and TAM requires a component-matching condition. Another valuable electronically tunable mixed-mode universal biquadratic filter structure with three CCCCTAs and two grounded capacitors was proposed in [27]. The circuit joins one more important advantage of orthogonal controllability of the resonance angular frequency (ω_o) and quality factor (Q) and enables implementation of all standard filtering functions in CM and TAM, but a component-matching condition is still needed to realise the AP response in TAM.

This study proposes a new configuration for realising electronically tunable mixed-mode universal biquadratic filters. The proposed circuit employs three CCCCTAs and two grounded capacitors. When operating in CM/TAM, the circuit can simultaneously realise LP, BP and HP filtering responses. The BS/AP filtering responses are also obtained with interconnection of the relevant output currents without any component-matching conditions. When operating in TIM, the circuit can simultaneously realise LP, HP and two BP filtering responses. The LP, BP, HP and BS/AP filtering responses are also obtained simultaneously in VM operation. The advantages of the proposed circuit are the following: (1) resistorless and electronically tunable structure; (2) simultaneous realisation of three generic filtering responses in all the four possible modes; (3) capability to realise BS and AP filtering responses in the VM, CM and TAM without critical component-matching conditions; (4) low-input and high-output impedances for current signals; (5) high-input impedance for voltage signal; (6) use of only grounded capacitors; (7) orthogonal control of the parameters Q and ω_o of the filter; (8) independent control of the VM filter gains without affecting the parameters Q and ω_o; and (9) low active and passive sensitivity performances. Tables 1 and 2 compare the proposed circuit with previously reported mixed-mode biquad circuits. It is interesting to note that the proposed circuit only employs three multiple-output CCCCTA active components and two grounded capacitors. Regarding the CCCCTA-based biquads proposed in [26,27], the proposed circuit does not require component-matching conditions to realise the AP response in CM and TAM, and two more standard filter signals can be obtained in VM. Another attractive feature is the independent tunability of the VM filter transfer gain constants without affecting the parameters ω_o and Q. Moreover, the CM filter enjoys a low-input and high-output impedance feature, which is a desirable feature for the CM cascading. Since the proposed circuit does not require external resistors and uses only grounded capacitors, it is suitable for integrated circuit (IC) implementation. Tables 3 and 4 compare the main features of the proposed circuit with those of previous CCCCTA-based works [26,27].

Table 1. Comparison of previously reported mixed-mode filters. [1]

Filters	No. of Active Elements	No. of Passive Elements	Composed of Equivalent Active Elements
[13]	7 CCII	2C + 8R	7 CCII
[14]	3 CCII	3C + 4R + 2 switch	3 CCII
[15]	4 CFOA	2C + 9R + 1 switch	4 CFOA
[16]	3 DVCC	2C + 3R	3 DVCC
[17]	3 DDCC	2C + 4R	3 DDCC
[18]	1 FDCCII	2C + 3R	2 DDCC
[19]	3 FTFN	2C + 3R	3 × 2 CFOA
[20]	7 OTA	2C	7 OTA
[21]	5 OTA	2C	5 OTA
[22]	4 OTA	2C	4 OTA
[23]	4 MOCCCII	2C	4 MOCCCII
[24]	5 MOCCCII	2C	5 MOCCCII
[25]	4 MOCCCII	2C	4 MOCCCII
[26]	3 CCCCTA	2C	3 × (1 CCCII + 1 OTA)
[27]	3 CCCCTA	2C	3 × (1 CCCII + 1 OTA)
this work	3 CCCCTA	2C	3 × (1 CCCII + 1 OTA)

[1] CCII: current conveyor; CFOA: current feedback operational amplifier; DVCC: differential voltage current conveyor; FDCCII: fully differential current conveyor; FTFN: four-terminal floating nullor; OTA: operational transconductance amplifier; MOCCCII: multiple-output current controlled conveyor; CCCCTA: current controlled current conveyor transconductance amplifier.

Table 2. Characteristic comparisons with previous reported mixed-mode filters.

Filters	Properties [1]								
	(1)	(2)	(3)	(4)	(5)	(6)	(7)	(8)	(9)
[13]	no	no	no	no	no	yes	yes	yes	yes
[14]	no	no	no	no	no	yes	no	yes	yes
[15]	no	no	no	no	no	yes	no	yes	yes
[16]	no	no	no	yes	yes	yes	yes	no	yes
[17]	no	yes	no	no	no	yes	yes	no	yes
[18]	no	no	no	no	no	yes	yes	no	no
[19]	no	no	no	no	no	no	no	no	yes
[20]	yes	no	no	no	yes	yes	yes	yes	yes
[21]	yes	no	no	no	yes	yes	yes	no	yes
[22]	yes	no	no	no	yes	yes	no	no	yes
[23]	yes	no	no	yes	yes	yes	no	no	yes
[24]	yes	yes	no	no	no	yes	yes	no	yes
[25]	yes	yes	no	yes	no	yes	no	no	yes
[26]	yes	yes	no	no	yes	yes	no	no	yes
[27]	yes	yes	no	yes	yes	yes	yes	no	yes
this work	yes	yes	yes	yes	yes	yes	yes	yes	yes

[1] (1) resistorless and electronically tunable structure; (2) simultaneous realisation of three generic filtering responses in all the four possible modes; (3) capability to realise bandstop and allpass filtering responses in the voltage mode, current mode and transadmittance mode without critical component-matching conditions; (4) low-input and high-output impedances for current signals; (5) high-input impedance for voltage signal; (6) use of only grounded capacitors; (7) orthogonal control of the parameters quality factor (Q) and resonance angular frequency (ω_o) of the filter; (8) independent control of the voltage mode filter gains without affecting the parameters Q and ω_o; and (9) low active and passive sensitivity performances.

Table 3. Comparison of the proposed circuit with previously reported single-input-type of electronically tunable CCCCTA-based mixed-mode filters [26,27]. [1]

Related Works	No. of Active Elements	Filter Function Realization				The ω_o and Q Orthogonal Tunability	Independent Tunability VM Filter Gains without Affecting ω_o and Q
		CM	VM	TAM	TIM		
[26]	3	All five	LP, BP, HP	All five	LP, BP, HP	no	no
[27]	3	All five	LP, BP, BS	All five	LP, BP, BS	yes	no
this work	3	All five	All five	All five	LP, BP, HP	yes	yes

[1] ω_o: resonance angular frequency; Q: quality factor; CM: current mode; VM: voltage mode; TAM: transadmittance mode; TIM: transimpedance mode; LP: lowpass; BP: bandpass; HP: highpass; BS: bandstop.

Table 4. Characteristic comparisons with previous works in [26,27]. [1]

Related Works	Matching Constraints	Input Voltage at High Input Impedance	Input Current at Low Input Impedance	Output Current at High Output Impedance
[26]	AP	yes	no	yes
[27]	AP	yes	yes	yes
this work	nil	yes	yes	yes

[1] AP: allpass.

2. Circuit Descriptions

2.1. Basic Concept and Implementation of the CCCCTA

The CCCCTA simplifies circuit implementation by providing an active building block. The CCCCTA device is obtained by cascading the CCCII with the OTA to implement analogue function circuits in compact monolithic chips [28,29]. This versatile component also has potential applications in analogue signal-processing circuits. Because its parasitic resistance and transconductance can be adjusted electronically by the input bias currents I_S and I_B, respectively, it does not require a resistor in practical applications, which is an attractive feature for filter designers. Figure 1 shows the circuit symbol of the CCCCTA [29]. The port relations of CCCCTA can be characterized by the following matrix equation [26–29]:

$$\begin{bmatrix} I_Y \\ V_X \\ I_{Z+} \\ I_{Z-} \\ I_O \\ I_{-O} \end{bmatrix} = \begin{bmatrix} 0 & 0 & 0 & 0 & 0 & 0 \\ R_X & 1 & 0 & 0 & 0 & 0 \\ 1 & 0 & 0 & 0 & 0 & 0 \\ -1 & 0 & 0 & 0 & 0 & 0 \\ 0 & 0 & g_m & 0 & 0 & 0 \\ 0 & 0 & -g_m & 0 & 0 & 0 \end{bmatrix} \begin{bmatrix} I_X \\ V_Y \\ V_{Z+} \\ V_{Z-} \\ V_O \\ V_{-O} \end{bmatrix} \tag{1}$$

where R_x and g_m are the parasitic resistance at X-terminal and the transconductance gain of the CCCCTA, respectively. The parasitic resistance R_x can be controlled by the bias current I_S of CCCCTA, and the transconductance gain g_m can be controlled by the bias current I_B of CCCCTA.

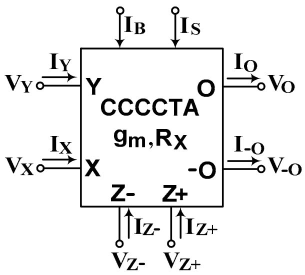

Figure 1. CCCCTA (current controlled current conveyor transconductance amplifier) symbolic representation.

2.2. Proposed Electronically-Tunable Mixed-Mode Biquadratic Filter

Figure 2 shows that the proposed electronically tunable mixed-mode biquadratic filter employs three CCCCTAs and two grounded capacitors. The multiple current outputs of the CCCCTA are easily implemented by adding output branches to the CCCCTA. The input current of the circuit is applied to the X-terminal of the first CCCCTA, which has low input impedance. The output currents are obtained at high output impedance ports, which simplifies cascading in both CM and TAM operations. The input voltage of the circuit is applied to the Y-terminal of the third CCCCTA, which has high input impedance. Because the circuit has low input impedance and high output impedance for current signals and has high input impedance for voltage signal, it can be used in cascade for realizing higher-order filters [16]. Moreover, grounded capacitors are used in integrated circuits to cancel parasitic impedance effects of active elements [16]. Routine analysis of the circuit in Figure 2 reveals that the following four output voltages and five output currents can be obtained.

$$V_{o1} = \frac{-G_{X1}G_{X2}(I_{in} - G_{X3}V_{in})}{D(s)} \tag{2}$$

$$V_{o2} = \frac{-sC_1G_{X1}(I_{in} - G_{X3}V_{in})}{D(s)} \quad (3)$$

$$V_{o3} = \frac{s^2C_1C_2(I_{in} - G_{X3}V_{in})}{D(s)} \quad (4)$$

$$V_{o4} = (\frac{1}{g_{m3}})\frac{sC_1g_{m1}G_{X1}I_{in} + G_{X3}(s^2C_1C_2G_{X1} + g_{m2}G_{X1}G_{X2})V_{in}}{D(s)} \quad (5)$$

$$I_{o1} = \frac{s^2C_1C_2G_{X1}(I_{in} - G_{X3}V_{in})}{D(s)} \quad (6)$$

$$I_{o2} = \frac{-sC_1g_{m1}G_{X1}(I_{in} - G_{X3}V_{in})}{D(s)} \quad (7)$$

$$I_{o3} = \frac{g_{m2}G_{X1}G_{X2}(I_{in} - G_{X3}V_{in})}{D(s)} \quad (8)$$

$$I_{o4} = \frac{sC_1g_{m1}G_{X1}I_{in} + G_{X3}(s^2C_1C_2G_{X1} + g_{m2}G_{X1}G_{X2})V_{in}}{D(s)} \quad (9)$$

$$I_{o5} = \frac{sC_1g_{m1}G_{X1}(I_{in} - G_{X3}V_{in})}{D(s)} \quad (10)$$

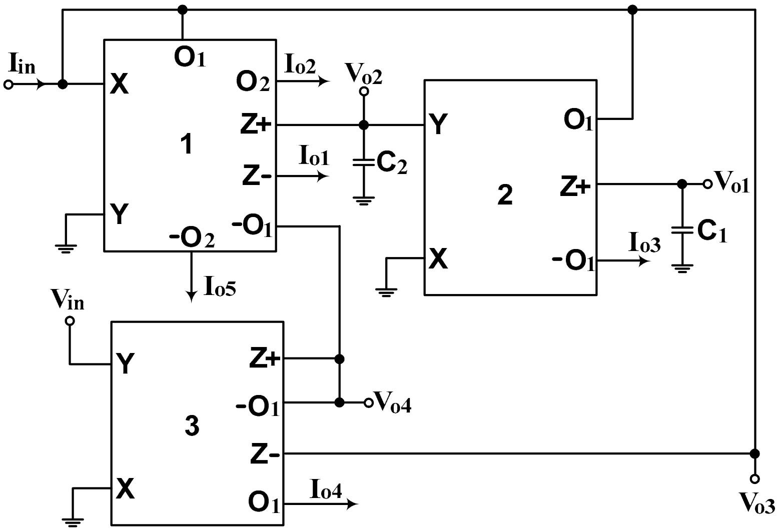

Figure 2. Proposed electronically tunable mixed-mode biquadratic filter.

D(s) is given by

$$D(s) = s^2C_1C_2G_{X1} + sC_1g_{m1}G_{X1} + g_{m2}G_{X1}G_{X2} \quad (11)$$

where $G_{X1} = \frac{1}{R_{X1}}$, $G_{X2} = \frac{1}{R_{X2}}$, and $G_{X3} = \frac{1}{R_{X3}}$.

2.2.1. CM and TIM

According to Equations (2)–(10), CM and TIM can be obtained by setting the input voltage V_{in} = 0 (grounded) and getting I_{in} as input signal. The five current transfer functions obtained are:

$$\frac{I_{o1}}{I_{in}} = \frac{s^2C_1C_2G_{X1}}{D(s)} \quad (12)$$

$$\frac{I_{o2}}{I_{in}} = \frac{-sC_1 g_{m1} G_{X1}}{D(s)} \tag{13}$$

$$\frac{I_{o3}}{I_{in}} = \frac{g_{m2} G_{X1} G_{X2}}{D(s)} \tag{14}$$

$$\frac{I_{o4}}{I_{in}} = \frac{I_{o5}}{I_{in}} = \frac{sC_1 g_{m1} G_{X1}}{D(s)} \tag{15}$$

Equations (12)–(15) indicate that a non-inverting HP filtering response is obtained from I_{o1}, an inverting BP filtering response is obtained from I_{o2}, a non-inverting LP filtering response is obtained from I_{o3}, and two non-inverting BP filtering responses are obtained from I_{o4} and I_{o5}. The BS filtering response is easily obtained by adding the two currents I_{o1} and I_{o3} to obtain the following transfer function:

$$\frac{I_{BS}}{I_{in}} = \frac{I_{o1} + I_{o3}}{I_{in}} = \frac{s^2 C_1 C_2 G_{X1} + g_{m2} G_{X1} G_{X2}}{D(s)} \tag{16}$$

Similarly, the AP transfer function is easily obtained by adding the three currents I_{o1}, I_{o2} and I_{o3} to obtain the following transfer function:

$$\frac{I_{AP}}{I_{in}} = \frac{I_{o1} + I_{o2} + I_{o3}}{I_{in}} = \frac{s^2 C_1 C_2 G_{X1} - sC_1 g_{m1} G_{X1} + g_{m2} G_{X1} G_{X2}}{D(s)} \tag{17}$$

Thus, all five standard filtering responses are provided by the same CM biquadratic filter structure, and no other component-matching conditions are needed. Notably, all current outputs are available from high-output impedance terminals. High-output impedance terminals of the configuration enable the circuit to be cascaded without additional current buffers. Because the gain of the current-mode HP, LP and BP filters is unity, the additional current amplifiers are needed if a variable gain of current-mode filter is necessary. In addition, the BS and AP filters cannot be realised simultaneously with the HP, LP and BP filters. This problem can be solved by adding the multiple current outputs that can be easily implemented by simply adding output branches.

According to Equation (11), filter parameters ω_o and Q are:

$$\omega_o = \sqrt{\frac{g_{m2} G_{X2}}{C_1 C_2}},\ Q = \frac{1}{g_{m1}} \sqrt{\frac{g_{m2} G_{X2} C_2}{C_1}} \tag{18}$$

Based on Equation (18), parameter Q can be independently tuned by using g_{m1} without disturbing ω_o. Restated, parameters ω_o and Q are orthogonally adjustable through the finite input conductance G_{X2} and then the g_{m1} in that order. This property is desirable in biquadratic filters because it increases design and tuning flexibility.

Accordingly, the four TIM transfer functions in this case can be obtained as follows:

$$\frac{V_{o1}}{I_{in}} = \frac{-G_{X1} G_{X2}}{D(s)} \tag{19}$$

$$\frac{V_{o2}}{I_{in}} = \frac{-sC_1 G_{X1}}{D(s)} \tag{20}$$

$$\frac{V_{o3}}{I_{in}} = \frac{s^2 C_1 C_2}{D(s)} \tag{21}$$

$$\frac{V_{o4}}{I_{in}} = \left(\frac{1}{g_{m3}}\right) \frac{sC_1 g_{m1} G_{X1}}{D(s)} \tag{22}$$

As indicated by Equations (19)–(22), an inverting LP filtering response is obtained from V_{o1}, an inverting BP filtering response is obtained from V_{o2}, a non-inverting HP filtering response is obtained from V_{o3}, and a non-inverting BP filtering response is obtained from V_{o4}. That is, the circuit provides TIM HP, LP and two BP responses simultaneously without disturbing circuit topology.

2.2.2. VM and TAM

According to Equations (2)–(10), VM and TAM can be obtained by setting the input voltage $I_{in} = 0$ (opened) and getting V_{in} as input signal. The four voltage transfer functions obtained are:

$$\frac{V_{o1}}{V_{in}} = \frac{G_{X1}G_{X2}G_{X3}}{D(s)} \tag{23}$$

$$\frac{V_{o2}}{V_{in}} = \frac{sC_1G_{X1}G_{X3}}{D(s)} \tag{24}$$

$$\frac{V_{o3}}{V_{in}} = \frac{-s^2C_1C_2G_{X3}}{D(s)} \tag{25}$$

$$\frac{V_{o4}}{V_{in}} = (\frac{G_{X3}}{g_{m3}})(\frac{s^2C_1C_2G_{X1} + g_{m2}G_{X1}G_{X2}}{D(s)}) \tag{26}$$

As indicated by Equations (23)–(26), a non-inverting LP filtering response is obtained from V_{o1}, a non-inverting BP filtering response is obtained from V_{o2}, an inverting HP filtering response is obtained from V_{o3}, and a non-inverting BS filtering response is obtained from V_{o4}. Notably, connecting the output current signal I_{o5} to the output voltage node V_{o4} also obtains a non-inverting AP transfer function in VM as follows:

$$\frac{V_{o4}}{V_{in}} = (\frac{G_{X3}}{g_{m3}})(\frac{s^2C_1C_2G_{X1} - sC_1g_{m1}G_{X1} + g_{m2}G_{X1}G_{X2}}{D(s)}) \tag{27}$$

The gain constants in Equations (23)–(26) are

$$H_{o1} = \frac{G_{X3}}{g_{m2}},\ H_{o2} = \frac{G_{X3}}{g_{m1}},\ H_{o3} = -\frac{G_{X3}}{G_{X1}},\ H_{o4} = \frac{G_{X3}}{g_{m3}} \tag{28}$$

In Equation (18), the proposed filter orthogonally controls ω_o and Q by tuning conductance G_{X2} for ω_o and then tuning transconductance gain g_{m1} for Q without disturbing parameter ω_o. According to Equation (28), the VM filter transfer gains can be independently controlled by changing G_{X3} without affecting ω_o and Q, and the finite input conductance G_{X3} at the X-terminal of the CCCCTA(3) is tunable. Therefore, the VM filter provides orthogonal tunability of all three filter parameters (ω_o, Q and H_o) in all five responses. This is because the three output voltages V_{o1}, V_{o2} and V_{o4} are not in low-output impedance terminals. Voltage followers are needed for the proposed circuit to drive low impedance loads or to be directly connected to the next stages.

Accordingly, the five TAM transfer functions in this case are obtained as follows:

$$\frac{I_{o1}}{V_{in}} = \frac{-s^2C_1C_2G_{X1}G_{X3}}{D(s)} \tag{29}$$

$$\frac{I_{o2}}{V_{in}} = \frac{sC_1g_{m1}G_{X1}G_{X3}}{D(s)} \tag{30}$$

$$\frac{I_{o3}}{V_{in}} = \frac{-g_{m2}G_{X1}G_{X2}G_{X3}}{D(s)} \tag{31}$$

$$\frac{I_{o4}}{V_{in}} = \frac{s^2C_1C_2G_{X1}G_{X3} + g_{m2}G_{X1}G_{X2}G_{X3}}{D(s)} \tag{32}$$

$$\frac{I_{o5}}{V_{in}} = \frac{-sC_1g_{m1}G_{X1}G_{X3}}{D(s)} \tag{33}$$

As indicated by Equations (29)–(33), an inverting HP filtering response is obtained from I_{o1}, a non-inverting BP filtering response is obtained from I_{o2}, an inverting LP filtering response is obtained from I_{o3}, a non-inverting BS filtering response is obtained from I_{o4} and an inverting BP filtering response is obtained from I_{o5}. Thus, the proposed filter can simultaneously realise LP, BP, HP and BS responses in TAM. The TAM AP transfer function is easily obtained by adding currents I_{o4} and I_{o5}, which yields the following transfer function:

$$\frac{I_{AP}}{V_{in}} = \frac{I_{o4} + I_{o5}}{V_{in}} = \frac{s^2 C_1 C_2 G_{X1} G_{X3} - s C_1 g_{m1} G_{X1} G_{X3} + g_{m2} G_{X1} G_{X2} G_{X3}}{D(s)} \tag{34}$$

Table 5 summarizes the four possible modes of the transfer functions according to Equations (2)–(10).

Table 5. Input conditions and various functions realised.

Filter function	V_{in} = 0, I_{in} is Input Signal		I_{in} = 0, V_{in} is Input Signal	
	CM	**TIM**	**VM**	**TAM**
HP	I_{o1}	V_{o3}	V_{o3}	I_{o1}
LP	I_{o3}	V_{o1}	V_{o1}	I_{o3}
BP	I_{o2}, I_{o4}, I_{o5}	V_{o2}, V_{o4}	V_{o2}	I_{o2}, I_{o5}
BS	I_{o1} + I_{o3}	—	V_{o4}	I_{o4}
AP	I_{o1} + I_{o2} + I_{o3}	—	V_{o4} *	I_{o4} + I_{o5}

* A non-inverting AP voltage-mode transfer function is easily obtained by connecting the output current signal I_{o5} to the output voltage node V_{o4}.

2.3. Non-Ideal Analysis and Sensitivity Performance

If the non-idealities of CCCCTA are considered, the relationships of the terminal voltages and currents can be rewritten as $V_X = \beta V_Y + I_X R_X$, $I_{Z+} = \alpha_p I_X$, $I_{Z-} = -\alpha_n I_X$, $I_{O1} = \gamma_p g_m V_{Z+}$, $I_{-O1} = -\gamma_n g_m V_{Z+}$, $I_{O2} = \eta_p g_m V_{Z+}$ and $I_{-O2} = -\eta_n g_m V_{Z+}$, where β, α_p, α_n, γ_p, γ_n, η_p and η_n are CCCCTA transfer ratios that deviate from unity by the transfer errors [27]. In a non-ideal case with reanalysis of the proposed circuit in Figure 2, the denominator of the non-ideal voltage transfer function is yielded as follows:

$$D(s) = \beta_1 s^2 C_1 C_2 G_{X1} + \alpha_{p1} \beta_1 \gamma_{p1} s C_1 g_{m1} G_{X1} + \alpha_{p1} \alpha_{p2} \beta_1 \beta_2 \gamma_{p2} g_{m2} G_{X1} G_{X2} \tag{35}$$

where β_i, α_{pi} and γ_{pi} are the parameters β, α_p and γ_p, respectively, of the ith CCCCTA (i = 1, 2, 3).

The non-ideal expressions for ω_o and Q are obtained as follows:

$$\omega_o = \sqrt{\frac{\alpha_{p1} \alpha_{p2} \beta_2 \gamma_{p2} g_{m2} G_{X2}}{C_1 C_2}},\ Q = \frac{1}{\gamma_{p1} g_{m1}} \sqrt{\frac{\alpha_{p2} \beta_2 \gamma_{p2} g_{m2} G_{X2} C_2}{\alpha_{p1} C_1}} \tag{36}$$

The active and passive sensitivities of the proposed circuit are

$$S^{\omega_o}_{\alpha_{p1}} = S^{\omega_o}_{\alpha_{p2}} = S^{\omega_o}_{\beta_2} = S^{\omega_o}_{\gamma_{p2}} = S^{\omega_o}_{g_{m2}} = S^{\omega_o}_{G_{X2}} = -S^{\omega_o}_{C_1} = -S^{\omega_o}_{C_2} = \frac{1}{2} \tag{37}$$

$$S^{Q}_{\alpha_{p2}} = S^{Q}_{\beta_2} = S^{Q}_{\gamma_{p2}} = S^{Q}_{g_{m2}} = S^{Q}_{G_{X2}} = S^{Q}_{C_2} = -S^{Q}_{\alpha_{p1}} = -S^{Q}_{C_1} = \frac{1}{2} \tag{38}$$

$$S^{Q}_{\gamma_{p1}} = S^{Q}_{g_{m1}} = -1 \tag{39}$$

These calculation results indicate that all sensitivities are low and have absolute values no larger than unity. The proposed circuit thus exhibited low sensitivity.

2.4. Effect of the CCCCTA Parasitic Impedances and Design Considerations

Next, various parasitic impedances of the CCCCTA in the proposed circuit were studied. Figure 3 represents the non-ideal CCCCTA model including its parasitic elements. A port Y parasitic is in the form $R_{Yi}//C_{Yi}$, a port Z+ parasitic is in the form $R_{Zi+}//C_{Zi+}$, a port Z− parasitic is in the form $R_{Zi-}//C_{Zi-}$, a port O_1 parasitic is in the form $R_{O1i}//C_{O1i}$, a port O_2 parasitic is in the form $R_{O2i}//C_{O2i}$, a port –O_1 parasitic is in the form $R_{-O1i}//C_{-O1i}$, a port –O_2 parasitic is in the form $R_{-O2i}//C_{-O2i}$, and a port X parasitic is in the form R_{Xi} where i = 1, 2, 3 and indicates the ith CCCCTA. After applying the non-ideal equivalent circuit mode of the CCCCTA in the proposed circuit, the denominator of the transfer functions becomes:

$$D(s) = \frac{m}{R_{3p}}s^2 + n_2 g_{m1} s + n_1 n_2 g_{m2} \tag{40}$$

where,

$$n_1 = (\frac{1}{R_{X2}})\frac{sR_{1p}}{1 + sR_{1p}C_1'} = (\frac{1}{R_{X2}C_1'})(\frac{s}{s + \omega_1}),\ \omega_1 = \frac{1}{R_{1p}C_1'} \tag{41}$$

$$n_2 = (\frac{1}{R_{X1}})\frac{sR_{2p}}{1 + sR_{2p}C_2'} = (\frac{1}{R_{X1}C_2'})(\frac{s}{s + \omega_2}),\ \omega_2 = \frac{1}{R_{2p}C_2'} \tag{42}$$

$$m = 1 + sR_{3p}C_{3p} = \frac{1}{\omega_3}(s + \omega_3),\ \omega_3 = \frac{1}{\frac{1}{R_{3p}C_{3p}}} \tag{43}$$

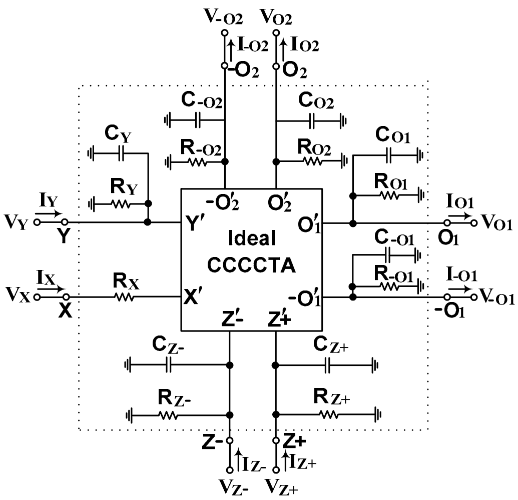

Figure 3. Non-ideal equivalent circuit model of the CCCCTA.

$C_1' = C_1//C_{Z2+}$, $C_2' = C_2//C_{Z1+}//C_{Y2}$, $C_{3P} = C_{O11}//C_{O12}//C_{Z3-}$, $R_{1p} = R_{Z2+}$, $R_{2p} = R_{Z1+}//R_{Y2}$, and $R_{3p} = R_{X1}//R_{O11}//R_{O12}//R_{Z3-}$.

Equations (41)–(43) illustrate that the effects of parasitic elements depend on three parasitic poles yielded by the non-idealities of CCCCTAs. For near-ideal frequency operation, the operating frequency must be higher than ω_1 and ω_2 and lower than ω_3. Therefore, the useful frequency range of the proposed filter is limited by the following conditions:

$$10 \times \max\{\omega_1, \omega_2\} << \omega << 0.1\omega_3 \tag{44}$$

This condition is easily satisfied since the external capacitance can be set much higher than the parasitic capacitance. In Figure 2, the effects of CCCCTA parasitic elements on the proposed filter can be ignored under the following conditions: min (C_1, C_2) >> parasitic capacitances (C_{Z1+}, C_{Z2+}, C_{Y2}), parasitic resistances (R_{O11}, R_{O12}, R_{Z3-}) >> R_{X1}, $1/sC_1$ << R_{Z2+} and $1/sC_2$ << $R_{Z1+}//R_{Y2}$.

According to (44), the effects of parasitic elements on coefficients n_1, n_2 and m diminish under the conditions $|s| >> \omega_1$, $|s| >> \omega_2$ and $|s| << \omega_3$. Hence,

$$n_1 \approx \frac{1}{R_{X2}C_1'} \tag{45}$$

$$n_2 \approx \frac{1}{R_{X1}C_2'} \tag{46}$$

$$m \approx 1 \tag{47}$$

By substituting Equations (45)–(47) into Equation (40) and assuming that (R_{O11}, R_{O12}, R_{Z3-}) >> R_{X1}, the characteristic equation is:

$$D(s) = s^2C_1'C_2'G_{X1} + sC_1'g_{m1}G_{X1} + g_{m2}G_{X1}G_{X2} \tag{48}$$

In this case, ω_o and Q become:

$$\omega_o = \sqrt{\frac{G_{X2}g_{m2}}{C_1'C_2'}},\ Q = \frac{1}{g_{m1}}\sqrt{\frac{G_{X2}g_{m2}C_2'}{C_1'}} \tag{49}$$

Thus, the effects of CCCCTA parasitic elements on the proposed filter in Figure 2 can be ignored in this case.

3. Simulation Results

3.1. Pre-Layout Simulation

The performance of the proposed circuit was evaluated by an H-Spice simulation in a Taiwan Semiconductor Manufacturing Company (TSMC) 0.18-µm process. Figure 4 shows the complementary metal oxide semiconductor (CMOS) implementation of a CCCCTA [29]. The multiple current outputs are easily implemented by simply adding output branches. Table 6 gives the dimensions of the metal oxide semiconductor (MOS) transistors used in the CCCCTA implementation. The supply voltages are $V_{DD} = -V_{SS}$ = 0.9 V. To obtain a pole frequency of f_o = 3.183 MHz at Q = 1, the active and passive components were set to $I_{B1} = I_{B2} = I_{B3}$ = 24.135 µA (g_m = 100 µS), $I_{S1} = I_{S2} = I_{S3}$ = 1.778 µA (R_X = 10 kΩ) and $C_1 = C_2$ = 5 pF. Figure 5 represents the simulated frequency responses for the HP (I_{o1}), BP (I_{o2}), LP (I_{o3}) and BP (I_{o4}) filters in the CM. Figure 6 represents the simulated frequency responses for the LP (V_{o1}), BP (V_{o2}), HP (V_{o3}) and BS (V_{o4}) filters, respectively, in the VM. Figure 7 represents the VM non-inverting AP (V_{o4}) simulated frequency response when the output current signal I_{o5} is connected to the output voltage node V_{o4}. Figure 8 represents the simulated frequency responses for the HP, BP, LP and BS filters in the TAM. Figure 9 represents the simulated frequency responses for the LP, BP, HP and BS filters in the TIM. Figure 10 represents VM gain responses of BP (V_{o2}) filter for different I_{B1} and I_{S3} values, by keeping $I_{B2} = I_{B3}$ = 24.135 µA, $I_{S1} = I_{S2}$ = 1.778 µA and $C_1 = C_2$ = 5 pF. The Q varied (1, 2, 5 and 10) when f_o was maintained at 3.183 MHz. Table 7 gives the different I_{B1} and I_{S3} values used in Figure 10. The Table 7 shows that Q can be used to adjust the input bias current I_{B1} without affecting the f_o as depicted in Equation (18) and that the BP (V_{o2}) transfer gains can be independently controlled by changing I_{S3} without affecting the f_o. Figure 11 represents the VM gain responses of the BP filter. The I_B and I_S values were changed by maintaining a constant ratio for constant Q. Table 8 shows the component values and corresponding ideal and simulated pole frequencies. The calculation results show that the f_o can be adjusted without affecting the Q. The input dynamic range of the VM filter was tested by repeating the simulation for a sinusoidal input signal at f_o = 3.183 MHz. Figure 12a shows the input dynamic range of the BP filter at the V_{o2} output terminal with $I_{B1} = I_{B2} = I_{B3}$ =96.5 µA (g_m = 200 µS), $I_{S1} = I_{S2} = I_{S3}$ = 7.113 µA (R_X = 5 kΩ) and $C_1 = C_2$ = 10 pF, which extended to an amplitude of 0.5 V (peak to peak) without signification distortion. In Figure 12a, the percentage of total harmonic distortion (THD) is 2.16%, and the total power dissipation is 1.99 mW. The dependence of the output harmonic distortion on input voltage amplitude is illustrated in Figure 12b.

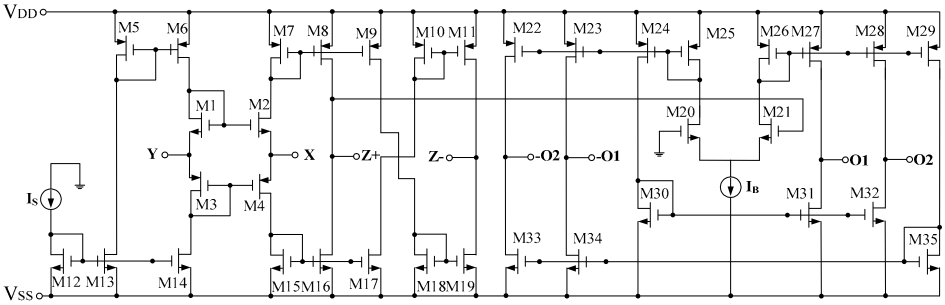

Figure 4. Complementary metal oxide semiconductor (CMOS) realization of the CCCCTA [29].

Table 6. The aspect ratios of the CMOS transistors in CCCCTA implementation.

Transistors	Length (µm)	Width (µm)
M1–M2	0.18	5
M3–M4	0.18	8
M5–M11	0.18	5
M12–M19	0.18	3
M20–M21	0.5	10
M22–M29	0.8	25
M30–M35	0.8	8

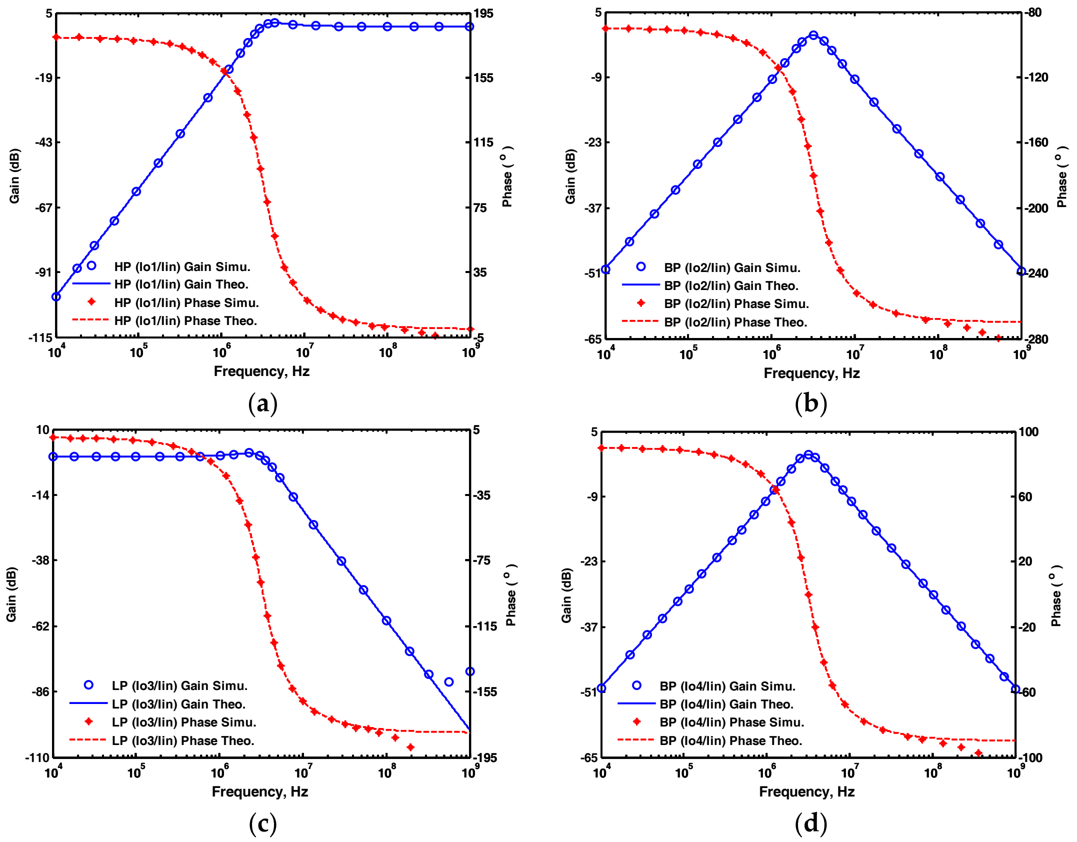

Figure 5. The CM-simulated frequency responses of Figure 2 (**a**) highpass filter; (**b**) bandpass filter; (**c**) lowpass filter; and (**d**) bandpass filter.

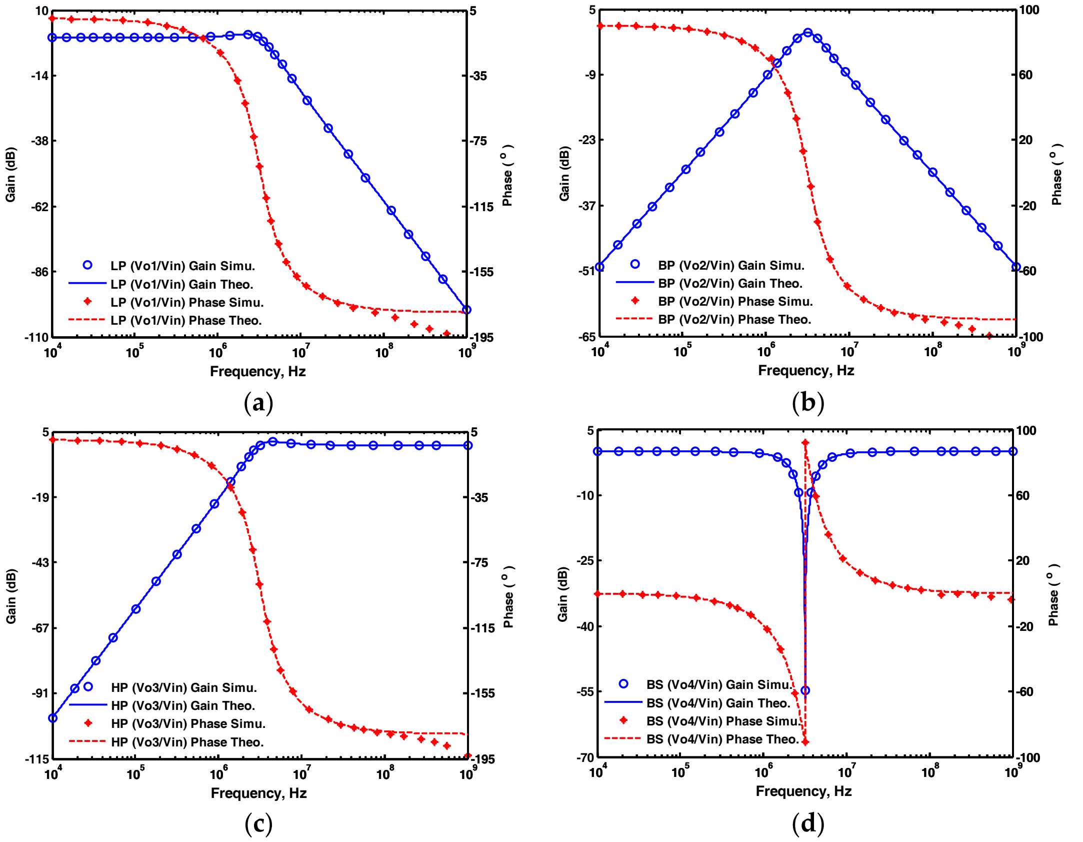

Figure 6. The VM-simulated frequency responses of Figure 2 (**a**) lowpass filter; (**b**) bandpass filter; (**c**) highpass filter; and (**d**) bandstop filter.

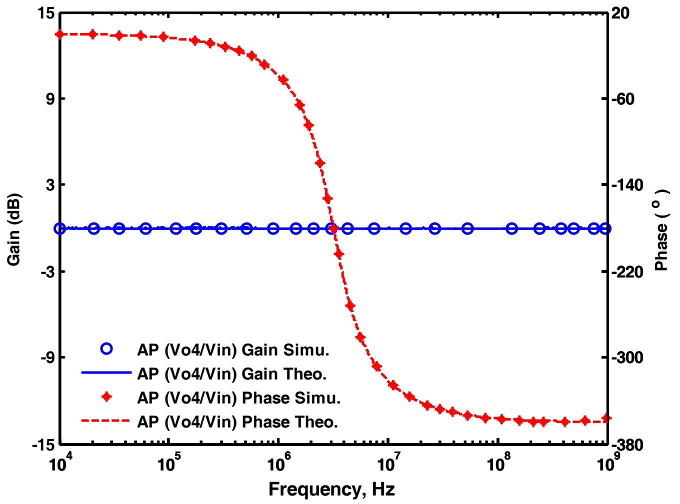

Figure 7. The VM-simulated allpass filter frequency responses of Figure 2.

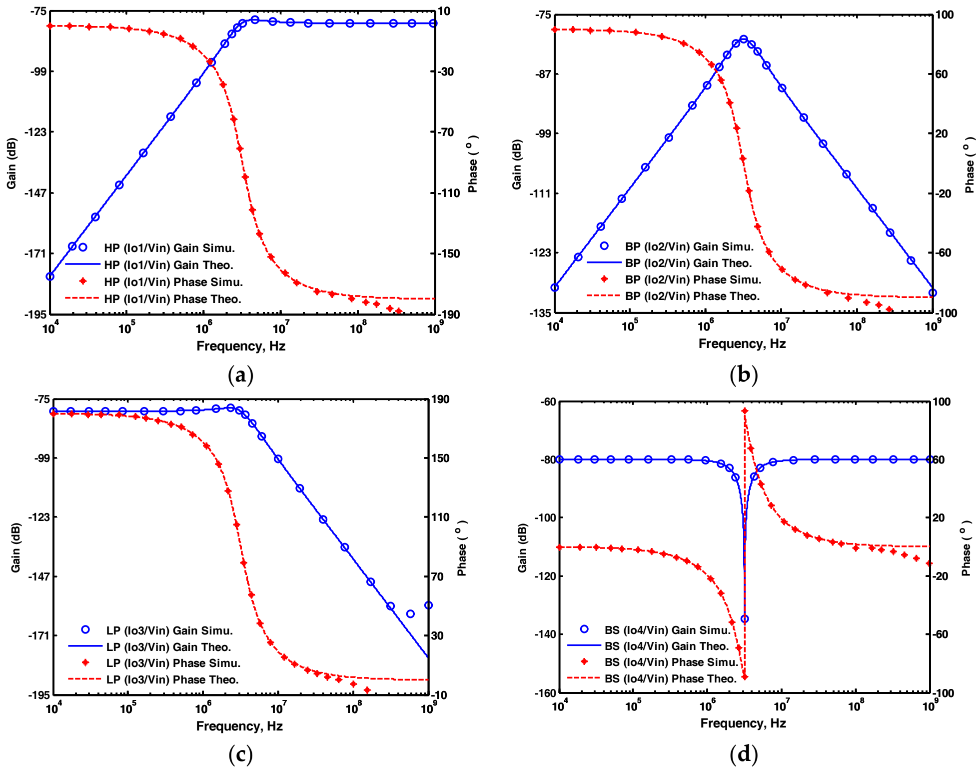

Figure 8. The TAM-simulated frequency responses of Figure 2 (**a**) highpass filter; (**b**) bandpass filter; (**c**) lowpass filter; and (**d**) bandstop filter.

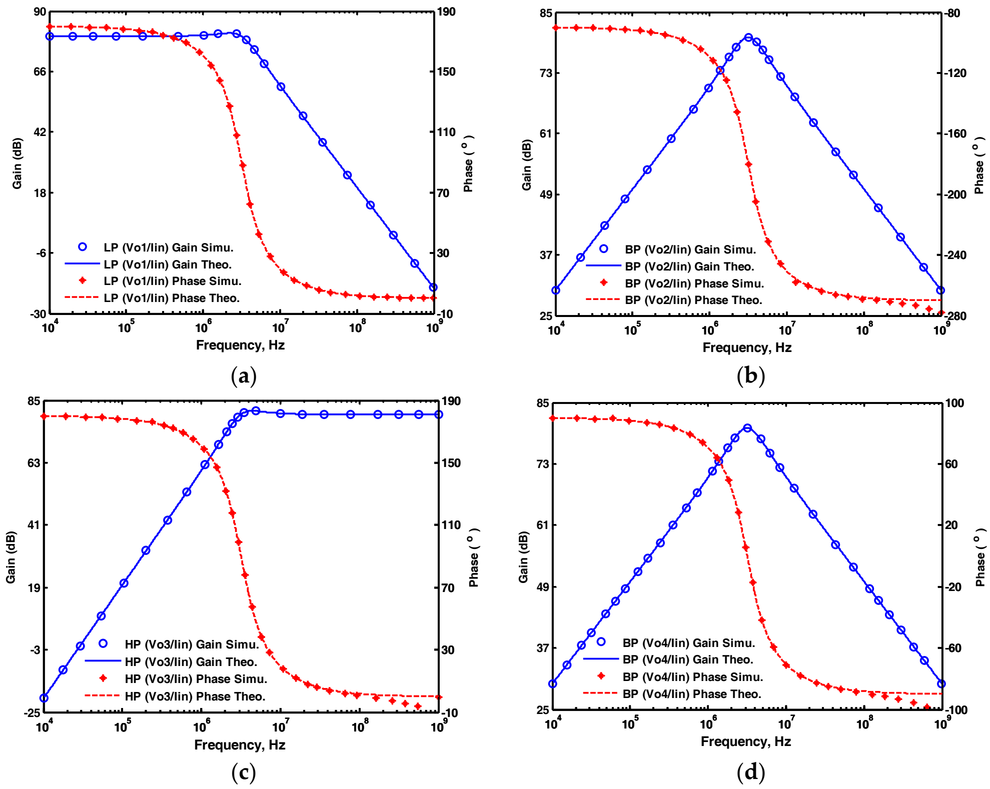

Figure 9. The TIM-simulated frequency responses of Figure 2 (**a**) lowpass filter; (**b**) bandpass filter; (**c**) highpass filter; and (**d**) bandpass filter.

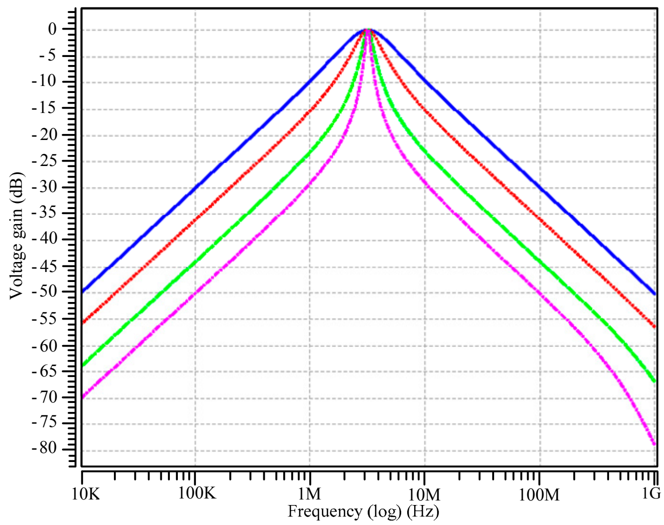

Figure 10. The VM bandpass filter at the output V_{o2} of Figure 2 when variation in Q with f_o fixed at 3.183 MHz (Q = 1: blue; Q = 2: red; Q = 5: green; and Q = 10: pink).

Table 7. The different I_{B1} and I_{S3} values used to obtain a specified *Q*.

Bias Current I_{B1} (μA)	Bias Current I_{S3} (μA)	Quality Factor
24.135	1.7782	Q = 1
6.035	0.4446	Q = 2
0.966	0.0712	Q = 5
0.241	0.0178	Q = 10

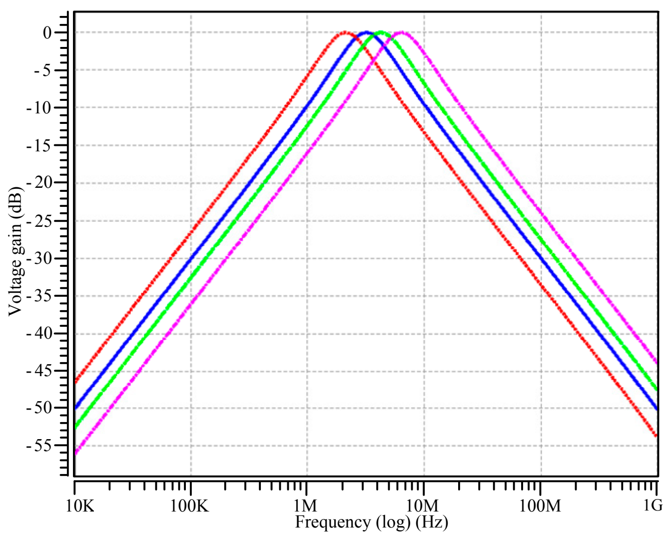

Figure 11. The VM bandpass filter at the output V_{o2} of Figure 2 when variation in f_o with Q fixed at 1 (f_o = 2.13 MHz: red; f_o = 3.22 MHz: blue; f_o = 4.32 MHz: green; and f_o = 6.48 MHz: pink).

Table 8. Component values used to obtain a specified f_o.

Bias Currents $I_{B1} = I_{B2} = I_{B3}$	Bias Currents $I_{S1} = I_{S2} = I_{S3}$	Capacitances $C_1 = C_2$	Calculated Value of f_o	Simulated Value of f_o	Frequency Error
10.726 µA (g_m = 66.67 µS)	0.79 µA (R_X = 15 kΩ)	5 pF	2.122 MHz	2.13 MHz	0.3%
24.135 µA (g_m = 100 µS)	1.7782 µA (R_X = 10 kΩ)	5 pF	3.183 MHz	3.22 MHz	1.62%
42.902 µA (g_m = 133.33 µS)	3.161 µA (R_X = 7.5 kΩ)	5 pF	4.244 MHz	4.32 MHz	1.79%
96.5 µA (g_m = 200 µS)	7.113 µA (R_X = 5 kΩ)	5 pF	6.366 MHz	6.48 MHz	1.79%

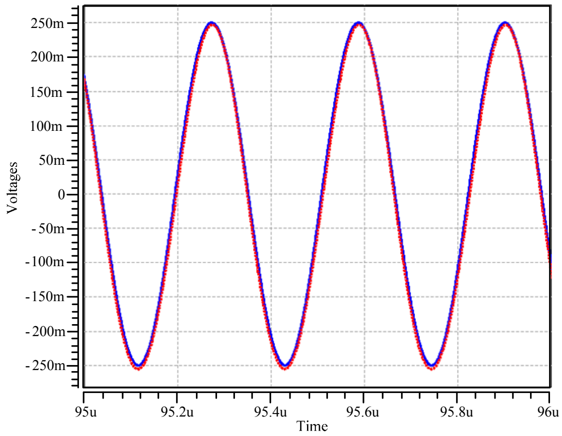

(**a**)

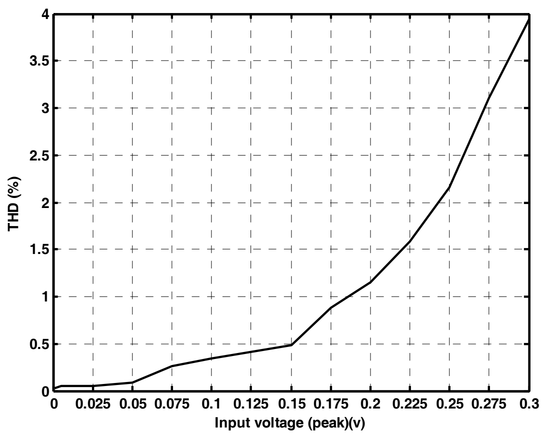

(**b**)

Figure 12. Time-domain results of VM bandpass filter at the output V_{o2} of Figure 2 (**a**) input (blue line) and output (red line) waveforms; (**b**) total harmonic distortion (THD) analysis results on input voltage at 3.183 MHz.

3.2. Post-Layout Simulation

The layout of the entire schematic was done using cadence's virtuoso tool. Figures 13 and 14 show the overall chip layout and the detail layout of the filter core, respectively. The layout floorplan is shown in Figure 15 which explains element placement. The component values of Figures 13 and 14 were given by g_m = 100 µS, R_X = 10 kΩ and $C_1 = C_2$ = 5 pF, leading to a center frequency f_o = 3.183 MHz. A design rules check (DRC) and a layout versus schematic (LVS) comparison were performed on the layout. The DRC checks for potential errors in the layout. The LVS checks the layout against the schematic and verifies that all the nets are matching. After the DRC and LVS were completed successfully, layout extraction was done. The extraction gives an overall idea about the parasitics of the design. All these processes are carried out using a cadence virtuoso schematic and layout editor tool for TSMC 0.18-µm CMOS process technology. The post-layout simulations were carried out to check the functionality of the design. Figure 16 represents the post-layout simulated frequency responses for the HP (I_{o1}), BP (I_{o2}), LP (I_{o3}) and BP (I_{o4}) filters in the CM. The post-layout simulation results show the CM simulated natural frequency as 3.10 MHz, that is, an approximately 2.52% error with the theoretical value. Figure 17 represents the post-layout simulated frequency responses for the LP (V_{o1}), BP (V_{o2}), HP (V_{o3}) and BS (V_{o4}) filter in the VM. The post-layout simulation results show the VM simulated natural frequency as 3.08 MHz, that is, an approximately 3.14% error with the theoretical value. Figure 18 represents the post-layout simulated frequency responses for the HP (I_{o1}), BP (I_{o2}), LP (I_{o3}) and BS (I_{o4}) filter in the TAM. The post-layout simulation results show the TAM simulated natural frequency as 3.10 MHz, that is, an approximately 2.52% error with the theoretical value. Figure 19 represents the post-layout simulated frequency responses for the LP (V_{o1}), BP (V_{o2}), HP (V_{o3}) and BP (V_{o4}) filter in the TIM. The post-layout simulation results show the TIM simulated natural frequency as 3.09 MHz, that is, an approximately 2.83% error with the theoretical value. It appears from Figures 16–19 that the filter post-layout simulation performs all the filter functions well, but the small departures filter responses mainly stems from the parasitic impedance effects and non-ideal gains of the CCCCTA. The total power dissipation is found to be 0.593 mW. The chip area without pads is only 0.5177×0.4507 mm^2.

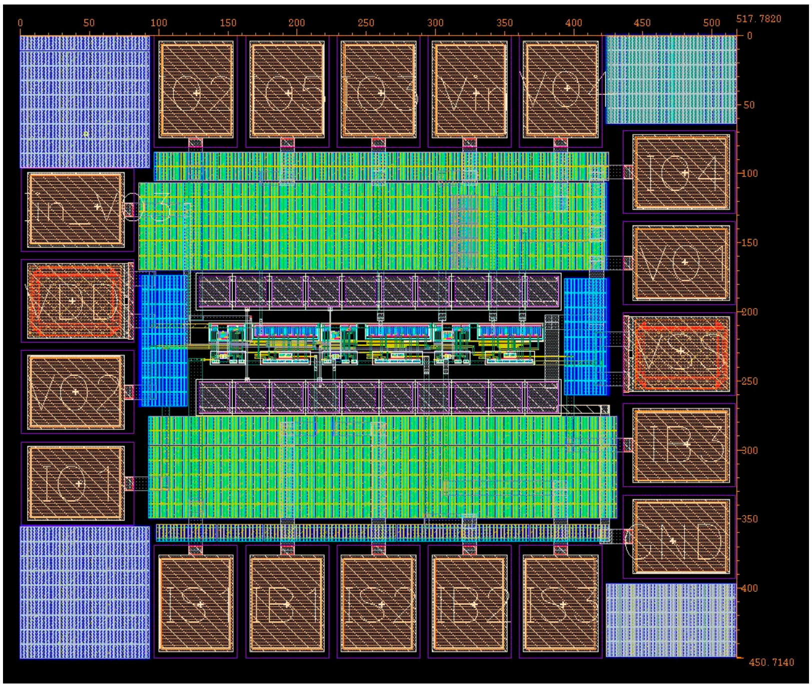

Figure 13. The layout of the proposed mixed-mode biquadratic filter chip.

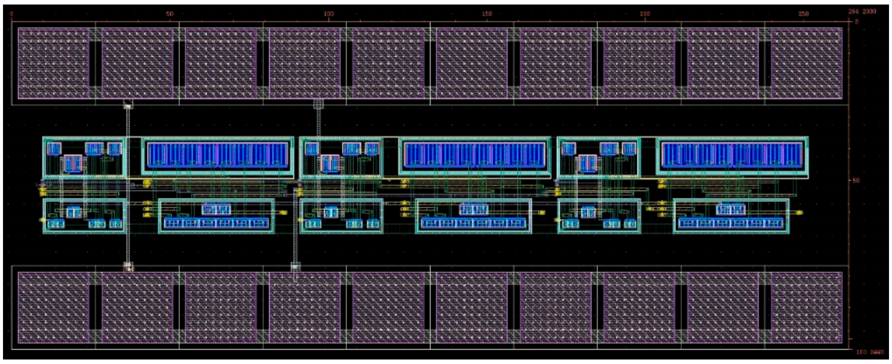

Figure 14. The core of the proposed mixed-mode biquadratic filter.

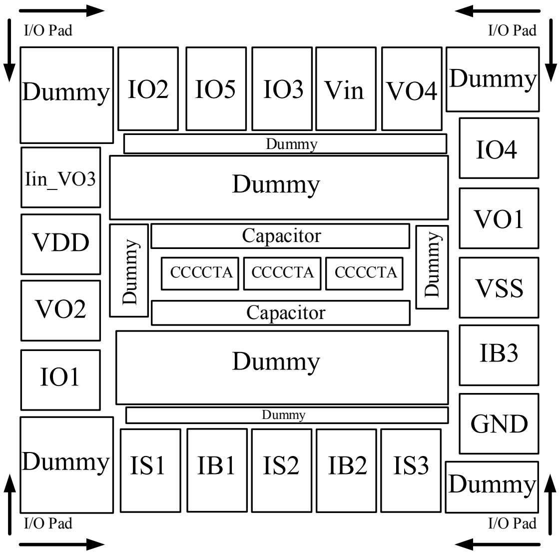

Figure 15. The layout floorplan.

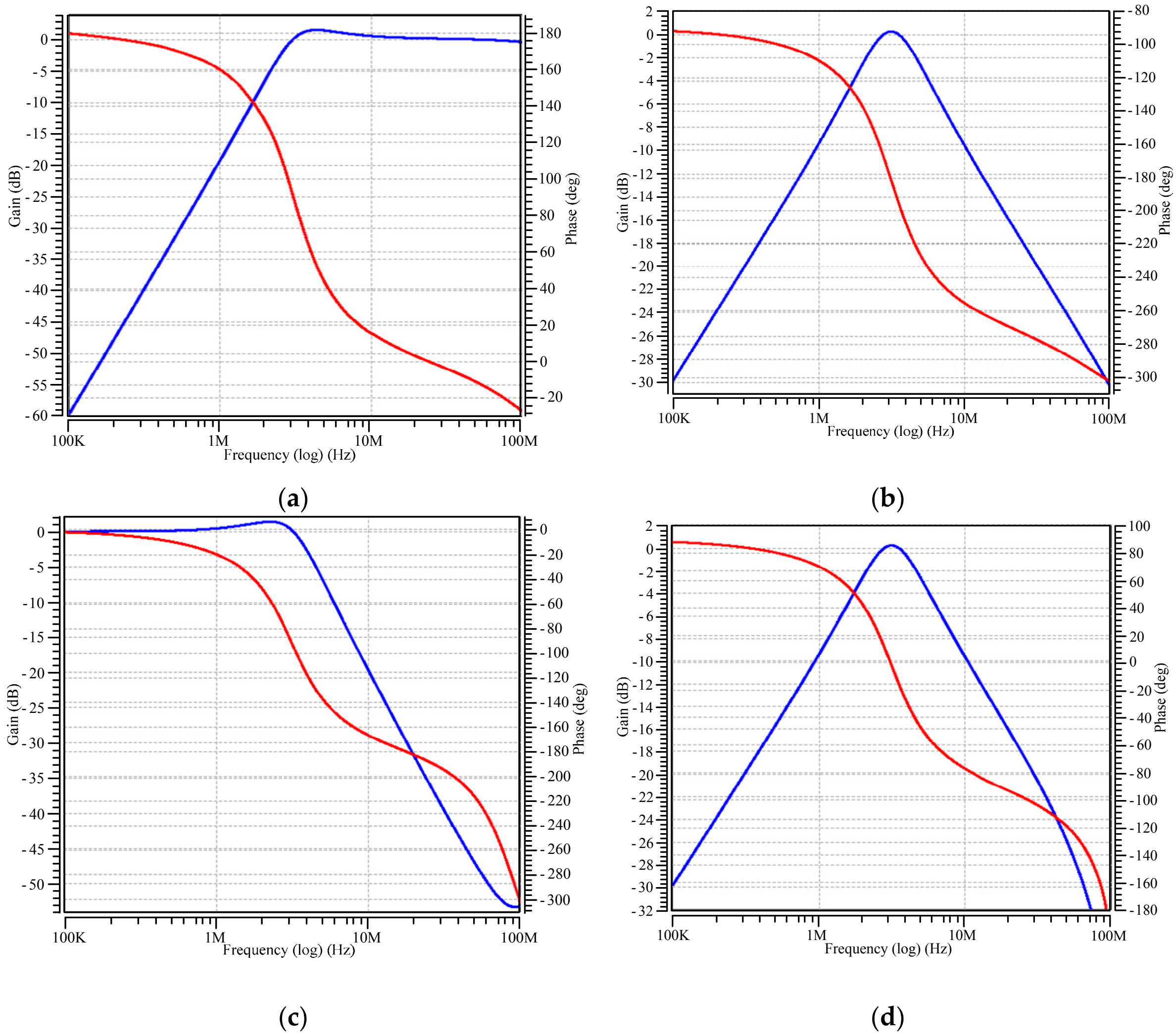

Figure 16. The CM post-layout gain (blue line) and phase (red line) simulation responses (**a**) highpass filter (I_{o1}/I_{in}); (**b**) bandpass filter (I_{o2}/I_{in}); (**c**) lowpass filter (I_{o3}/I_{in}),; and (**d**) bandpass filter (I_{o4}/I_{in}).

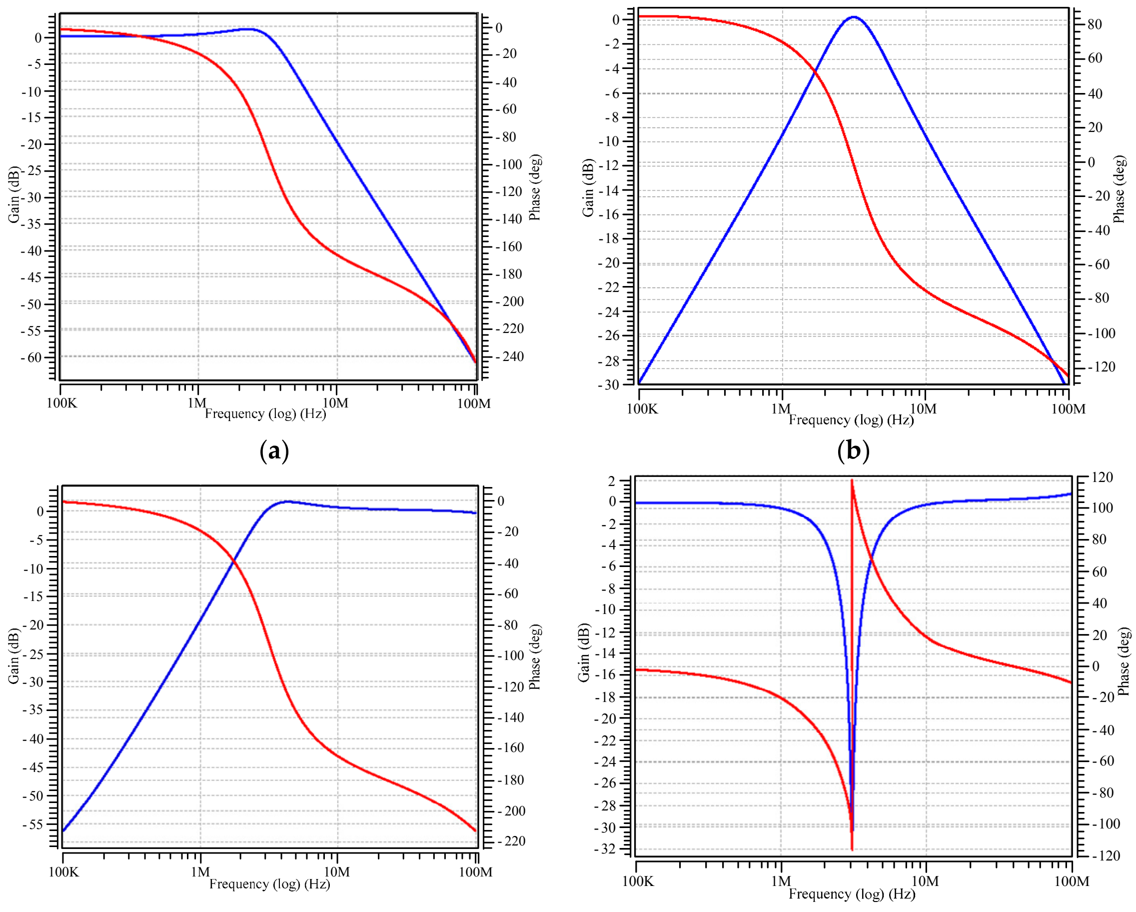

(**a**) (**b**)

(**c**) (**d**)

Figure 17. The VM post-layout gain (blue line) and phase (red line) simulation responses (**a**) lowpass filter (V_{o1}/V_{in}); (**b**) bandpass filter (V_{o2}/V_{in}); (**c**) highpass filter (V_{o3}/V_{in}); and (**d**) bandstop filter (V_{o4}/V_{in}).

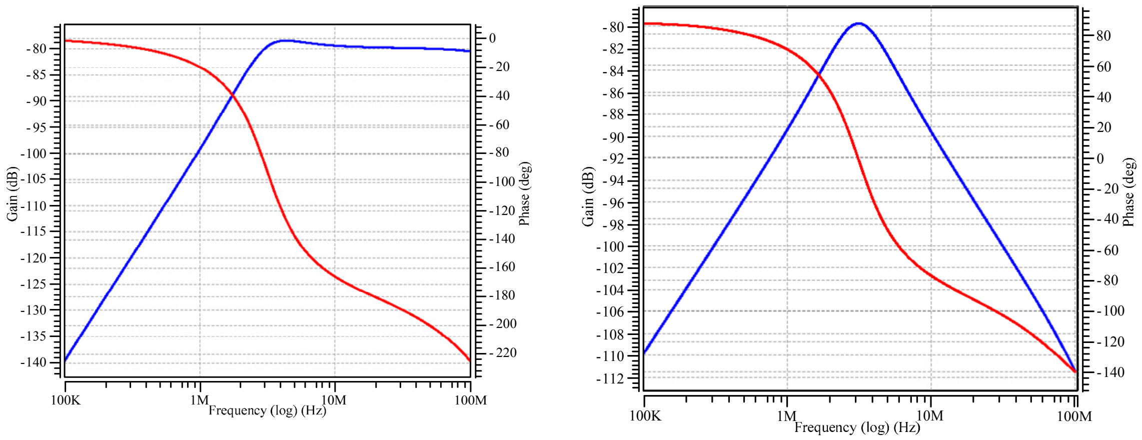

(**a**) (**b**)

Figure 18. *Cont.*

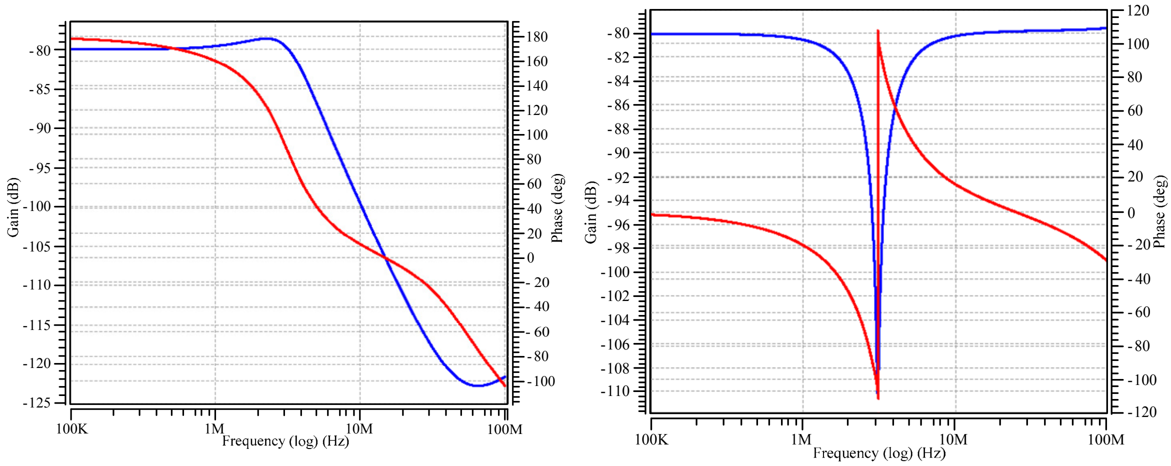

(**c**) (**d**)

Figure 18. The TAM post-layout gain (blue line) and phase (red line) simulation responses (**a**) highpass filter (I_{o1}/V_{in}); (**b**) bandpass filter (I_{o2}/V_{in}); (**c**) lowpass filter (I_{o3}/V_{in}); and (**d**) bandstop filter (I_{o4}/V_{in}).

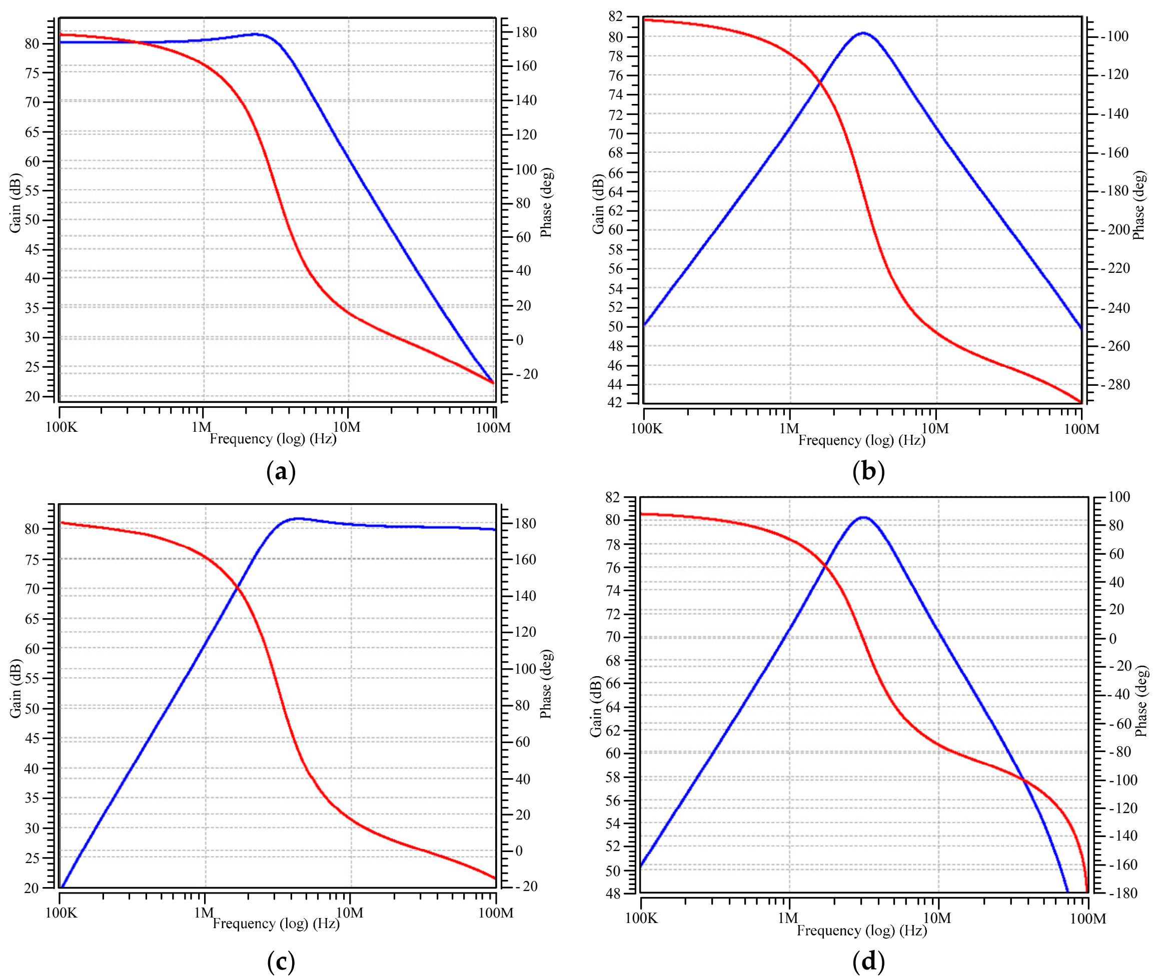

(**a**) (**b**)

(**c**) (**d**)

Figure 19. The TIM post-layout gain (blue line) and phase (red line) simulation responses (**a**) lowpass filter (V_{o1}/I_{in}); (**b**) bandpass filter (V_{o2}/I_{in}); (**c**) highpass filter (V_{o3}/I_{in}); and (**d**) bandpass filter (V_{o4}/I_{in}).

4. Conclusions

This paper presents a new CCCCTA-based electronically tunable mixed-mode biquadratic filter, which uses three CCCCTAs and two grounded capacitors. When operating in CM/TAM, the circuit can simultaneously realise LP, BP and HP filtering responses. The BS/AP filtering responses are also obtained with the interconnection of the relevant output currents without any component-matching conditions. When operating in TIM, the circuit can simultaneously realise LP, HP and two BP filtering responses. The LP, BP, HP and BS/AP filtering responses are also obtained simultaneously in VM operation. The proposed circuit has the following nine advantages simultaneously: (1) resistorless and electronically tunable structure; (2) simultaneous realisation of three generic filtering responses in all the four possible modes; (3) capability to realise BS and AP filtering responses in the VM, CM and TAM without critical component-matching conditions; (4) low-input and high-output impedances for current signals; (5) high-input impedance for voltage signal; (6) use of only grounded capacitors; (7) orthogonal control of the parameters Q and ω_o of the filter; (8) independent control of the VM filter gains without affecting the parameters Q and ω_o; and (9) low active and passive sensitivity performances. The pre-layout simulation and post-layout simulation results in this study were consistent with the theoretical assumptions.

Acknowledgments: The authors would like to thank the reviewers and academic editor for their suggestions to improve the manuscript. Technical support from the National Chip Implementation Center (CIC) is also gratefully acknowledged.

Author Contributions: Hua-Pin Chen and Wan-Shing Yang conceived and designed the theoretical verifications; the optimization ideas were provided by Wan-Shing Yang; Hua-Pin Chen analysed the results and wrote the paper.

Conflicts of Interest: The authors declare no conflict of interest.

References

1. Wilson, B. Recent developments in current conveyors and current-mode circuits. *IEE Proc. G Circuits Devices Syst.* **1990**, *137*, 63–77. [CrossRef]
2. Schmid, H. Why "current mode" does not guarantee good performance. *Analog Integr. Circuits Signal Process.* **2003**, *35*, 79–90. [CrossRef]
3. Cicekoglu, O.; Tarim, N.; Kuntman, H. Wide dynamic range high output impedance current-mode multifunction filters with dual-output current conveyors. *AEU Int. J. Electron. Commun.* **2002**, *56*, 55–60. [CrossRef]
4. Chang, C.M.; Al-Hashimi, B.M.; Rose, J.N. Unified active filter baquad structures. *IEE Proc. Circuits Devices Syst.* **2004**, *151*, 273–277. [CrossRef]
5. Maheshwari, S. High input impedance VM-APSs with grounded passive elements. *IET Circuits Devices Syst.* **2007**, *1*, 72–78. [CrossRef]
6. Maheshwari, S. High output impedance current-mode all-pass sections with two grounded passive components. *IET Circuits Devices Syst.* **2008**, *2*, 234–242. [CrossRef]
7. Hwang, Y.S.; Liu, W.H.; Tu, S.H.; Chen, J.J. New building block: Multiplication-mode current conveyor. *IET Circuits Devices Syst.* **2009**, *3*, 41–48. [CrossRef]
8. Maheshwari, S. Analogue signal processing applications using a new circuit topology. *IET Circuits Devices Syst.* **2009**, *3*, 106–115. [CrossRef]
9. Maheshwari, S.; Mohan, J.; Chauhan, D.S. Voltage-mode cascadable all-pass sections with two grounded passive components and one active element. *IET Circuits Devices Syst.* **2010**, *4*, 113–122. [CrossRef]
10. Maheshwari, S.; Chaturvedi, B. High-input low-output impedance all-pass filters using one active element. *IET Circuits Devices Syst.* **2012**, *6*, 103–110. [CrossRef]
11. Abdalla, K.K.; Bhaskar, D.R.; Senani, R. Configuration for realizing a current-mode universal filter and dual-mode quadrature single resistor controlled oscillator. *IET Circuits Devices Syst.* **2012**, *6*, 159–167. [CrossRef]
12. Ibrahim, M.A.; Minaei, S.; Kuntman, H. A 22.5 MHz current-mode KHN-biquad using differential voltage current conveyor and grounded passive elements. *Int. J. Electron. Commun.* **2005**, *59*, 311–318. [CrossRef]

13. Abuelma'atti, M.T.; Bentrcia, A.; Al-Shahrani, S.M. A novel mixed-mode current-conveyor-based filter. *Int. J. Electron.* **2004**, *91*, 191–197. [CrossRef]
14. Pandey, N.; Paul, S.K.; Bhattacharyya, A.; Jain, S.B. A new mixed mode biquad using reduced number of active and passive elements. *IEICE Electron. Express* **2006**, *3*, 115–121. [CrossRef]
15. Singh, V.K.; Singh, A.K.; Bhaskar, D.R.; Senani, R. Novel mixed-mode universal biquad configuration. *IEICE Electron. Express* **2005**, *2*, 548–553. [CrossRef]
16. Minaei, S.; Ibrahim, M.A. A mixed-mode KHN-biquad using DVCC and grounded passive elements suitable for direct cascading. *Int. J. Circuits Theory Appl.* **2009**, *37*, 793–810. [CrossRef]
17. Liao, W.B.; GU, J.C. SIMO type universal mixed-mode biquadratic filter. *Indian J. Eng. Mater. Sci.* **2011**, *18*, 443–448.
18. Lee, C.N.; Chang, C.M. Single FDCCII-based mixed-mode biquad filter with eight outputs. *AEU Int. J. Electron. Commun.* **2009**, *63*, 736–742. [CrossRef]
19. Shah, N.A.; Malik, M.A. Multifunction mixed-mode filter using FTFNs. *Analog Integr. Circuits Process.* **2006**, *47*, 339–343. [CrossRef]
20. Abuelma'atti, M.T.; Bentrcia, A. A novel mixed-mode OTA-C universal filter. *Int. J. Electron.* **2005**, *92*, 375–383. [CrossRef]
21. Chen, H.P.; Liao, Y.Z.; Lee, W.T. Tunable mixed-mode OTA-C universal filter. *Analog Integr. Circuits Process.* **2009**, *58*, 135–141. [CrossRef]
22. Lee, C.N. Multiple-mode OTA-C universal biquad filters. *Circuits Syst. Signal Process.* **2010**, *29*, 263–274. [CrossRef]
23. Pandey, N.; Paul, S.K. Mixed-mode universal filter. *J. Circuits Syst. Comput.* **2013**, *22*, 1250064. [CrossRef]
24. Li, Z.J. Mixed-mode universal filter using MCCCII. *AEU Int. J. Electron. Commun.* **2009**, *63*, 1072–1075.
25. Pandey, N.; Paul, S.K. SIMO mixed mode universal filter. *J. Act. Passiv. Eletron. Devices* **2012**, *7*, 215–226.
26. Maheshwari, S.; Singh, S.V.; Chauhan, D.S. Electronically tunable low-voltage mixed-mode universal biquad filter. *IET Circuits Devices Syst.* **2011**, *5*, 149–158. [CrossRef]
27. Singh, S.V.; Maheshwari, S.; Chauhan, D.S. Novel electronically tunable mixed-mode biqaud filter. In *Electronics and Signal Processing, Lecture Notes in Electrical Engineering (LNEE)*; Springer: Berlin/Heidelberg, Germany, 2011; Volume 97, pp. 735–742.
28. Siripruchyanun, M.; Jaikla, W. Current controlled current conveyor transconductance amplifier (CCCCTA): A building block for analog signal processing. *Electr. Eng.* **2008**, *9*, 443–455. [CrossRef]
29. Jaikla, W.; Siripongdee, S.; Suwanjan, P. MISO current-mode biquad filter with independent control of pole frequency and quality factor. *Radioengineering* **2012**, *21*, 886–891.